



Strength and strain capacities of concrete compression members reinforced with FRP

G. Campione *, N. Miraglia

Dipartimento di Ingegneria, Strutturale e Geotecnica, Università di Palermo, Viale delle Scienze, 90128 Palermo, Italy

Received 15 March 2001; accepted 26 April 2001

Abstract

The analytical compressive behavior of concrete members reinforced with fiber-reinforced polymer (FRP) was examined. The variation in the shape of the transverse cross-section was analyzed. The bearing capacity and the increase in the maximum strain for members having a cross-section which was circular, square or square with round corners reinforced with FRP were determined. The proposed analytical model allows one to evaluate the confining pressure in ultimate conditions considering the effective confined cross-section and also allows one to determine the ultimate strain corresponding to FRP failure through a simplified energetic approach. Analytical results are then compared to experimental values available in the literature, showing good agreement. © 2001 Elsevier Science Ltd. All rights reserved.

Keywords: Fiber-reinforced polymer; Confinement; Compressive strength; Ultimate strain

1. Introduction

Several theoretical and experimental investigations [1,2] are concerned with calculating the strength and ductility of compressed concrete elements with traditional confinement steel reinforcements (spirals, hoops, stirrups) and having circular or rectangular transverse cross-section. These studies have shown that the presence of transverse steel reinforcement increases the bearing capacity of compressed members due to the triaxial stress state which arises in the concrete core. In structural members confined with steel spirals the maximum increase in bearing capacity and ductility is higher with respect to that obtained utilizing circular steel hoops and with respect to that obtained in square or rectangular sections.

More recently the interest in using composite material, like fiber-reinforced polymer (FRP), for retrofitting or strengthening of concrete structures, has led to the attention of researchers and of the industry on the topic of confinement due to the presence of FRP.

It was shown [3-13] that the use of FRP materials offers almost always an increase in strength and ductility, and also several advantages with respect to traditional concrete structures, like the non-corrodibility and the lightness of composite materials, and ease of application in real structures.

Focusing the attention on the behavior of compression members, the main parameters investigated in literature [3-13] are the type of FRP material (carbon, aramid, glass, etc.) and its manufacture (unidirectional or bi-directional wraps), the shape of the transverse cross-section of the members, the dimensions and the shape of specimens, the strength of concrete, the types and percentages of steel reinforcements.

As already observed for concrete members confined with steel transverse reinforcements, also in members reinforced with FRP there is a greater increase in strength [9] for members having circular transverse cross-section, compared to those having square or rectangular transverse cross-section, the latter showing in some cases no increase in strength due to the presence of FRP.

In the present investigation an analytical model to predict maximum strength and ultimate strain of concrete confined with FRP is proposed. Compression members having different shapes of transverse cross-sections, also in the presence of longitudinal steel rein-

*Corresponding author. Tel.: +39-091-656-8467; fax: +39-091-656-8407.

E-mail address: campione@stru.diseg.unipa.it (G. Campione).

Nomenclature			
A_a	area of longitudinal steel	k_1	concrete strength enhancement coefficient
A_c	area of core of section within centerlines of FRP perimeter	r	corner radius of cross-section
A_{cc}	area of core within centerlines of FRP perimeter excluding area of longitudinal steel	t	thickness of FRP layers
A_f	area of FRP in the cross-section	U_{cc}	ultimate strain energy per unit volume of confined concrete
b_d	concrete core dimension to centerline of FRP perimeter	U_{sl}	energy required to maintain yield in the longitudinal steel in compression
E_f	modulus of elasticity of FRP	U_{co}	ultimate strain energy per unit volume of unconfined concrete
E_0	initial concrete modulus of elasticity	U_{st}	ultimate energy per unit volume spent to break the composite FRP
f'_c	compressive strength of unconfined concrete	ε_{co}	strain at maximum stress of unconfined concrete
f'_{cc}	compressive strength (peak stress) of confined concrete	ε_{cf}	strain of FRP composite measured at failure on the middle of the side in the cross-section
f_y	yield stress of steel	ε_{cu}	ultimate concrete compressive strain defined as strain at FRP failure in tension
f_l	lateral confining stress on concrete core from FRP transverse reinforcement	ε_f	ultimate strain of FRP composite
f'_l	effective lateral confining stress	ε_{su}	strain of FRP composite
f_r	stress in FRP wraps	$\Delta\varepsilon$	increase in maximum strain
f_{st}	stress of FRP composite	μ	increase in maximum strain of FRP-confined concrete compared to that of unconfined concrete
f_u	ultimate strength of FRP	ρ_{cc}	ratio of longitudinal reinforcement A_a to the area of cross-section A_c
N_u	ultimate load of FRP confined compressed section	ρ_f	transverse FRP reinforcement ratio
k_c	confinement effectiveness coefficient		
k_i	reduction factor of FRP stress due to the shape of the cross-section		

62 forcements and confinement with FRP wraps are ana- 70
 63 lyzed. Lastly, the analytical results are compared with 71
 64 experimental results available in the literature [4,5,7– 72
 65 9,13] showing the good agreement achieved with the 73
 66 proposed model.

67 2. Strength of compression members reinforced with FRP

68 As already mentioned, the use of FRP materials in 74
 69 concrete compression members produces an increase in 75

76 strength depending on the FRP properties (material 71
 77 type, strength, thickness, etc.), on the concrete proper- 72
 78 ties, and prevalently on the shape of the transverse 73
 79 cross-section.

80 Fig. 1 shows typical stress–strain curves of compression 74
 81 tests carried out by the authors [13] on concrete 75
 82 specimens having a cross-section which is circular or 76
 83 square with slightly rounded corners reinforced with 77
 84 FRP wraps. The wrap type is unidirectional, one layer, 78
 85 high strength, high modulus carbon fiber having thick- 79
 86 ness $t = 0.165$ mm, modulus of elasticity $E_f = 230$ GPa, 80
 81 ultimate strength $f_u = 3430$ MPa and ultimate strain 81
 82 $\varepsilon_f = 1.5\%$. The volumetric ratio of FRP reinforcement 82
 83 utilized is $\rho_f = 0.668\%$ and it is defined as the volumetric 83
 84 ratio of FRP in the unit volume of concrete core equal 84
 85 to $\rho_f = A_f/A_c$, with A_f the area of the composite in the 85
 86 cross-section, and A_c the area of the cross-section. 86

87 It was observed [13] that the presence of FRP rein- 87
 88 forcement increases the strength of plain concrete, but 88
 89 this phenomenon is strongly influenced by the shape of 89
 90 the cross-section. 90

91 The effectiveness of FRP reinforcement is less in the 91
 92 case of a square section compared to a circular cross- 92
 93 section and this is due to the concentration of stresses 93
 94 at the corner of the square section and also to the smaller 94
 95 effectively confined concrete core in a square section 95

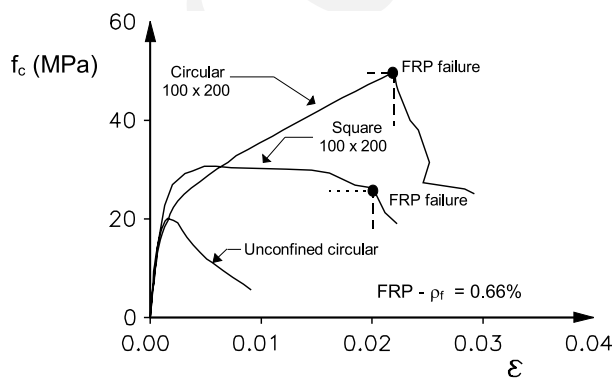


Fig. 1. Stress–strain curves for FRP-reinforced concrete specimens with different shapes of the transverse cross-section [13].

96 with respect to a circular cross-section. As a conse-
 97 quence of this, in order to obtain in columns having a
 98 square cross-section analogous performance in terms of
 99 strength as in columns having a circular transverse
 100 cross-section and reinforced with FRP, an increase in
 101 the volumetric ratio of FRP is required and/or a trans-
 102 formation of the square section into one with rounded
 103 corners, utilizing adequate corners radii. To do this it is
 104 possible to modify the shape of the square section, be-
 105 fore the application of FRP, by adding new concrete on
 106 the sides of the square section until the desired shape is
 107 obtained.

108 In the present investigation the effect of FRP on the
 109 confinement action in compression concrete members
 110 with variation in the shape of the transverse cross-sec-
 111 tion, shown in Fig. 2, is analyzed.

112 The cases of circular ($r = b_d/2$) and square ($r = 0$)
 113 sections form the limits of the square section with round
 114 corners.

115 In the following exposition, the attention is on the
 116 determination of the effective confinement pressure and
 117 on the determination of the effectively confined area of
 118 concrete core.

119 Experimental research [1] has shown that in the
 120 presence of a triaxial stress state the effective pressure
 121 determining failure of cylindrical concrete specimens is:

$$f'_{cc} = f'_c + k_1 f'_1, \quad (1)$$

123 f'_c being the ultimate cylindrical strength of plain con-
 124 crete, f'_1 the effective lateral pressure confining the con-
 125 crete core due to FRP and k_1 an experimental coefficient
 126 generally assumed for concrete [1] between 2.8 and 4.1.

127 The applicability of k_1 coefficient between 2.8 and 4.1
 128 for FRP reinforcement is limited [11] due to the inherent
 129 anisotropy in the composite materials. This would result
 130 in generally poor comparison between experimental and
 131 predict results especially as related to strain [11]. In the
 132 present study, using a regression analysis of the experi-
 133 mental data with a correlation factor of 88%, k_1 equal to
 134 2 was assumed for concrete members reinforced with
 135 FRP wraps.

136 The increase in strength due to the effective lateral
 137 pressure f'_1 depends on the lateral pressure f_1 assumed to
 138 be uniformly distributed over the surface of the concrete

core and also depends on the effectiveness coefficient k_e ,
 according to the following:

$$f'_1 = k_e f_1, \quad (2)$$

where

$$k_e = A_e / A_{cc} \quad (3)$$

with A_e the area of the effectively confined concrete core
 and A_{cc} the transverse area of concrete enclosed by the
 centerlines of the perimeter FRP defined as:

$$A_{cc} = A_c (1 - \rho_{cc}), \quad (4)$$

ρ_{cc} being the ratio of longitudinal reinforcement A_a to
 the area of cross-section A_c .

It is shown in the following exposition that both the
 coefficient k_e and the pressure f_1 depend on the shape of
 the cross-section of the compression members.

2.1. Determination of the effective lateral confining pressure

To determine the effective confinement pressure it is
 possible to refer to the rigid body equilibrium of the
 transverse cross-section (Fig. 3) subjected to the dis-
 tributed pressure f_1 and to the localized forces in the
 FRP in the ultimate condition.

The fundamental hypotheses assumed are:

- all transverse cross-sections of the members are in the same condition along the height of the members due to the presence of continuous FRP reinforcement;
- FRP behaves elastically up to failure and sudden failure occurs after the maximum strength is reached;
- perfect adhesion between concrete and FRP is ensured up to the failure of compression members.

It is important to observe that failure in tension of
 FRP wraps does not always occur; and the rupture of
 FRP occurs only when the compressive stress and the
 confining pressure, that are variable with the strain
 values, reach their maximum [11].

The analytical method here developed considers only
 the cases in which failure of FRP in tension occurs and
 further studies will be developed to extend the method
 to the cases in which FRP do not fail in tension.

In the case of a circular cross-section the stress in the
 fiber can be assumed to be uniform all along the pe-

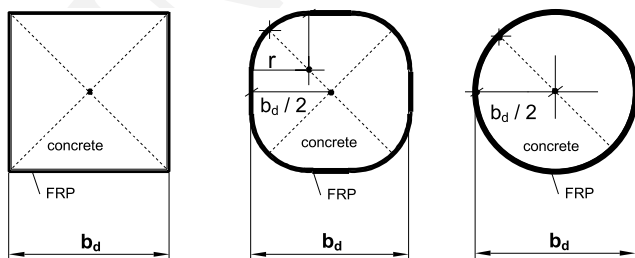


Fig. 2. Shapes of the cross-sections examined.

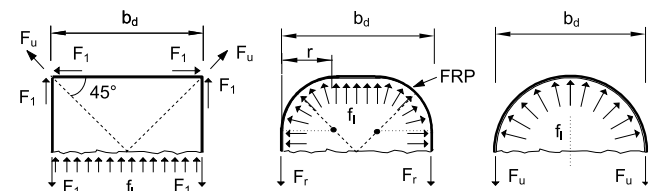


Fig. 3. Effective lateral confining pressure for FRP-reinforced cross-sections.

179 rimeter of the circumference; instead, in a square cross-
 180 section the stress is not uniform along the perimeter
 181 because of stress concentration near the corners of the
 182 section. In an approximate way this can be taken into
 183 account by considering a constant reduced uniform
 184 stress all along the perimeter equal to f_r , as shown in the
 185 following paragraph.

186 Because of the equilibrium of the forces in the FRP at
 187 the corners of the cross-section the maximum action
 188 acting in the direction parallel to the sides of the section
 189 is $0.707F_u = 0.707t f_u$. The coefficient 0.707 is obtained
 190 by considering that the resulting forces at the corners of
 191 the square section have the direction of the diagonal of
 192 the square section and because of the equilibrium of the
 193 forces the maximum value F_u allowed in the direction
 194 parallel to the sides of the square section is $F_1 = 0.707F_u$.

195 In the case of a square section with round corners the
 196 presence of round-filled corners reduces the concentra-
 197 tion of stresses at the corners, ensuring a more gradual
 198 variation in stress, with values between those related to
 199 the cases of circular and square cross-sections.

200 By considering, in a simplified way, the stress f_r in
 201 FRP variable with the radii of the corners r it is possible
 202 to obtain:

$$f_r = f_u \left[\left(1 - \frac{\sqrt{2}}{2} k_i \right) \frac{2r}{b_d} + k_i \frac{\sqrt{2}}{2} \right], \quad (5)$$

204 k_i being a reduction factor of the stress determined ex-
 205 perimentally and introduced in (5) to take into account
 206 the stress intensification in FRP at the corners. As it will
 207 be shown in the section relative to the comparison with
 208 the experimental data, assuming a constant value of k_i
 209 equal to 0.2121, a best fitting of experimental data was
 210 obtained with a correlation factor of 92%.

211 By considering the equilibrium of forces in the
 212 transverse cross-section shown in Fig. 3 subjected to
 213 internal confining pressure f_1 and to the concentrated
 214 forces at the free end of the FRP, it is possible to obtain
 215 the expressions of f_1 for the cases examined.

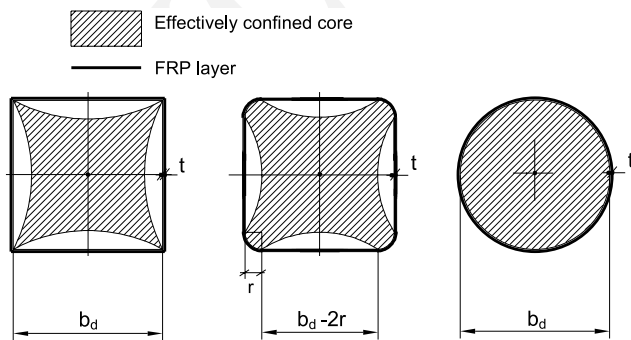


Fig. 4. Effective confined concrete core of cross-section reinforced with FRP.

For a cross-section which is circular, square with
 round corners or square we obtained:

$$f_1 = \frac{2t f_u}{b_d} \quad \text{circular}, \quad (6)$$

$$f_1 = \frac{2t f_r}{b_d} \quad \text{square with round corners}, \quad (7)$$

$$f_1 = \frac{\sqrt{2} t f_u}{b_d} k_i \quad \text{square}. \quad (8)$$

2.2. Effectiveness coefficient k_e

For the determination of the effectiveness factor k_e it
 can be assumed (see Fig. 4) that, in the case of a circular
 cross-section, the entire concrete core internal to the
 perimeter of FRP is effectively confined, while, for the
 square section there is a reduction in the effectively
 confined core that can be assumed, analogously with the
 case of concrete core confined by transverse steel stir-
 rups [1], in the form of a second-degree parabola with an
 initial tangent slope of 45° .

For the square section with round corners it can be
 assumed, as also suggested by experimental observation
 [13], that the presence of round corners produces at the
 corners a further effective confinement area with respect
 to the case of the square section, leading to a more ef-
 fective confined core represented by the area enclosed by
 the parabola and by the round corners, as shown in Fig.
 4. The effectively confined concrete core shown in Fig. 4
 is represented with the hatched area.

Based on this observation, it is possible to obtain the
 k_e factor that, for a square section with round corners,
 is:

$$k_e = \frac{[b_d^2 - 4(r^2 - \frac{\pi r^2}{4})] - \frac{2}{3}(b_d - 2r)^2}{b_d^2 - 4(r^2 - \frac{\pi r^2}{4})}. \quad (9)$$

This factor assumes values of $k_e = 1$ for a circular sec-
 tion and of $k_e = 1/3$ for a square section. The latter is in

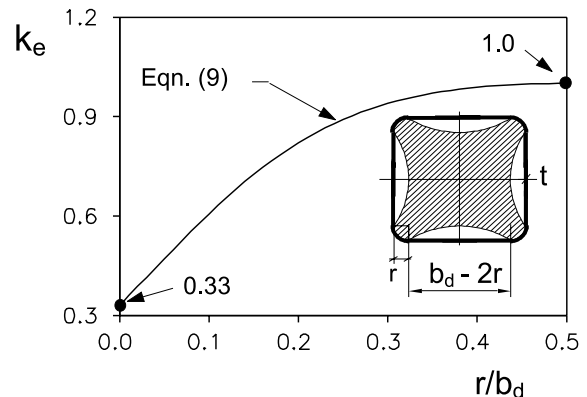


Fig. 5. Variation in the effectiveness coefficient k_e with r/b_d .

244 accordance with the hypothesis that the reduction in the
245 volume of effectively confined concrete is due only to the
246 reduction of effectively confined area of the transverse
247 cross-section.

248 Fig. 5 shows the variation in k_c with r/b_d . It is in-
249 teresting to observe that, for values of r/d_b above 0.2,
250 80% of the total transverse area of the cross-section is
251 effectively confined.

252 Having determined the effective lateral pressure f'_1 , it
253 is possible to evaluate the strength N_u of a compressed
254 member confined with FRP, also in the presence of
255 longitudinal steel reinforcements, utilizing the superpo-
256 sition principle and separately considering the contri-
257 bution due to the presence of FRP evaluated by using
258 (1) and the contribution due to the longitudinal steel of
259 area A_a assumed to have yielded, as follows:

$$N_u = f'_c A_c + f_y A_a + k_1 k_c f_1 A_c. \quad (10)$$

261 Fig. 6, for some values of the parameter r/b_d , shows the
262 variation in maximum strength f'_{cc} referred to that of
263 unconfined plain concrete f'_c with the parameter $\rho_f f_u / f'_c$
264 for the different section types examined. It is interesting
265 to observe that, to get a prefixed strength value, the
266 amount of volume percentages of FRP greatly depends
267 on the shape of the section. In particular a square sec-
268 tion reinforced with FRP having the same strength as a
269 circular section requires higher percentages of FRP,
270 which is not cheap at present.

271 3. Monotonical stress–strain relationship for compressed 272 members confined with FRP

273 For the analytical modeling of the complete com-
274 pressive stress–strain curves of FRP-confined members
275 the following relationship, which is also represented in
276 Fig. 7, can be utilized:

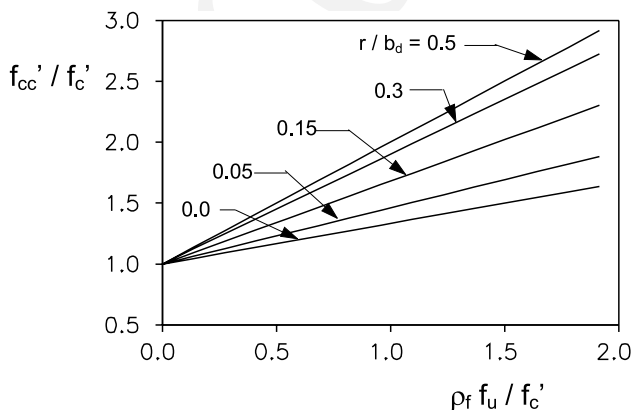


Fig. 6. Increase in the compressive strength with $\rho_f f_u / f'_c$.

$$\frac{f_c}{f'_c} = \beta \frac{\varepsilon}{\varepsilon_{co}} + \left\{ \left\{ (1 - \beta) \frac{\varepsilon}{\varepsilon_{co}} \right\} \right. \\ \left. / \left\{ \left[1 + \left(\frac{\varepsilon}{\varepsilon_{co}} \right)^R \right]^{1/R} \right\} \right\}, \quad (11)$$

where

$$\beta = \frac{E_h}{E_0}; \quad E_h = \frac{f'_{cc} - f'_c}{\varepsilon_{cu} - \varepsilon_{co}}. \quad (12)$$

This model is a revised version of the well-known Pinto and Giuffrè [14] model originally proposed for stress–strain curves of steel. The (11) relationship represents a curved transition from a straight line asymptote with slope E_0 , E_0 being the initial modulus of FRP concrete, to another asymptote with slope E_h . The β parameter is the strain hardening ratio, that is the ratio between E_h and E_0 and R is a parameter which influences the shape of the transition curve and here assumed constant and equal to 3 to reproduce with good approximation experimental results.

The hardening part is governed by the strength and by the maximum strain characteristics of confined and unconfined concrete. The stress–strain curve stops when the maximum stress f'_{cc} and maximum strain ε_{cu} are reached and FRP breaks in tension because its ultimate strain has been reached. The proposed equation for stress–strain curve (11), as it will shown in the following section relative to comparison which experimental data, fits very well the experimental data referring to the cases in with FRP produces strain-hardening in concrete specimens (i.e. for the case of cylindrical specimens), instead in the cases in which the increase of strength due to the presence of FRP is negligible (i.e. cases of square section), no good prediction is expected.

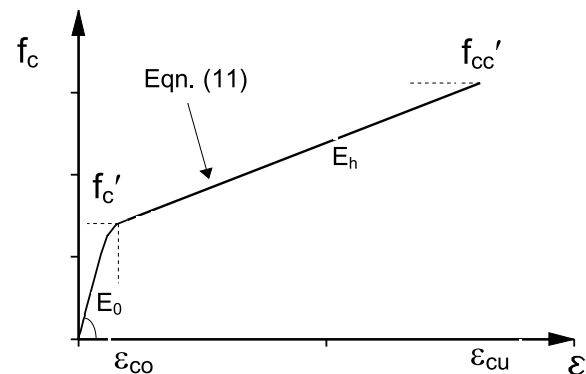


Fig. 7. Stress–strain model in compression for FRP confined concrete members.

305 **4. Ultimate concrete strain at FRP failure**

306 To determine the ultimate axial strain of confined
 307 concrete core ϵ_{cu} the well-known model proposed by
 308 Mander et al. [1] based on the energy balance approach
 309 was considered, though we also consider the contribu-
 310 tion due to the presence of FRP.

311 The energy balance equation can be written as fol-
 312 lows:

$$U_{st} = U_{cc} - U_{co} + U_{sl}, \quad (13)$$

314 where U_{st} is the ultimate strain energy per unit volume
 315 spent to break the composite FRP:

$$U_{st} = \rho_f A_c \int_0^{\epsilon_{us}} f_{st} d\epsilon_{st}. \quad (14)$$

317 U_{cc} is the ultimate strain energy per unit volume of
 318 confined concrete:

$$U_{cc} = A_c \int_0^{\epsilon_{cu}} f_c d\epsilon_c. \quad (15)$$

320 U_{co} is the ultimate strain energy per unit volume of
 321 unconfined concrete:

$$U_{co} = A_c \int_0^{2\epsilon_0} f_{uc} d\epsilon_c. \quad (16)$$

323 U_{sl} is the energy per unit volume required to maintain
 324 yield in the longitudinal steel in compression:

$$U_{sl} = \rho_{cc} A_c \int_0^{\epsilon_{cu}} f_{sl} d\epsilon_{sl}. \quad (17)$$

326 ϵ_{us} being the ultimate strain of the composite, f_{st} and ϵ_{st}
 327 the stress and the strain in the composite.

328 By substituting the expressions (14)–(17) into (13) it is
 329 possible, knowing the complete stress–strain relation-
 330 ship of materials, to obtain the ultimate strain of con-
 331 crete core ϵ_{cu} .

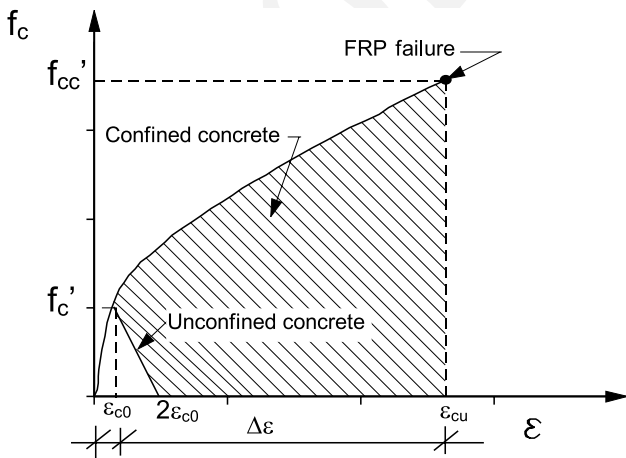


Fig. 8. Stress–strain model in compression for calculation of ultimate concrete strain.

In an approximate way it is possible to obtain the
 ultimate strain of the concrete core ϵ_{cu} knowing only the
 maximum strength of the unconfined and confined
 concrete core. As shown in Fig. 8, in the cases of both
 plain concrete and FRP confined concrete, the area
 subtended under the stress–strain curves represents the
 energy per unit volume spent to break the concrete in
 compression and corresponding to the strain values
 determining FRP failure in tension. If the contribution
 due to the longitudinal steel to maintain yield is ne-
 glected, to simplify the calculation, the difference be-
 tween the area subtended by the stress–strain curve of
 confined concrete less the area subtended under the
 stress–strain curves of the unconfined concrete repre-
 sents the energy spent to produce failure of FRP.

In this case the ultimate strain ϵ_{cu} can be obtained by
 the following:

$$\epsilon_{cu} = \epsilon_{co} + \Delta\epsilon. \quad (18)$$

By setting the area subtended under the f_c – ϵ diagram in
 compression (Fig. 8) equal to the internal work per-
 formed to break the FRP in tension through the cross-
 section of the confined concrete core, it is possible to
 obtain the increase in strain $\Delta\epsilon$ and hence the maximum
 strain ϵ_{cu} . The energy per unit volume of confined con-
 crete can be calculated approximately as the area of the
 trapezium having sides f'_{cc} and f'_c and base $\Delta\epsilon$.

This approximation is validated by the following
 considerations: the shape of the effective stress–strain
 curve f_c – ϵ due to the presence of FRP is approximately
 linear after f'_c is reached; the area subtended up to the f'_c
 of the unconfined concrete is negligible compared to the
 other quantities.

The energy spent to break the FRP wraps, having
 area of the transverse cross-section A_f , can be evaluated
 exactly by using (13) and setting the two above-men-
 tioned areas equal as follows:

$$\frac{1}{2} \Delta\epsilon (f'_{cc} + f'_c) A_c = A_f \frac{1}{E_f} f_r^2, \quad (19)$$

which gives the increase in maximum strain $\Delta\epsilon$:

$$\Delta\epsilon = 2 \rho_f \frac{f_r^2}{E_f} \frac{1}{2 f'_c + k_1 k_e f_1} \quad \text{with} \quad (20)$$

$$\rho_f = \frac{2 [2 (b_d - 2r) + \pi r] t}{b_d^2 - 4 (r^2 - (\pi r^2 / 4))}$$

or in extended form

$$\Delta\epsilon = \frac{2 f_r^2}{E_f} \frac{[2 (b_d - 2r) + \pi r] t}{b_d^2 - 4 (r^2 - (\pi r^2 / 4))} \left\{ 1 / \left\{ f'_c + k_1 \frac{t}{b_d} f_r \right. \right. \\ \left. \left. \times \frac{[b_d^2 - 4 (r^2 - \frac{\pi r^2}{4})] - \frac{2}{3} (b_d - 2r)^2}{b_d^2 - 4 (r^2 - \frac{\pi r^2}{4})} \right\} \right\}. \quad (21)$$

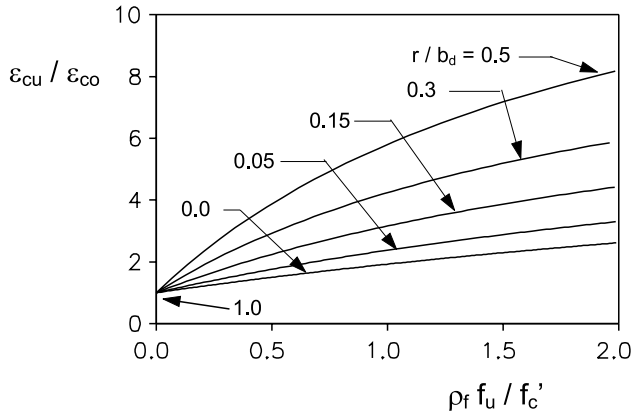


Fig. 9. Increase in the ultimate strain with $\rho_f f_u / f'_c$.

373 Assuming $k_1 = 2$, as already mentioned in accordance
 374 with experimental data, the increase, $\mu = (\varepsilon_{co} + \varepsilon) / \varepsilon_{co}$, in
 375 maximum strain of FRP confined concrete compared to
 376 that of unconfined concrete is

$$\mu = 1 + \rho_f \frac{1}{\varepsilon_{co}} \frac{f_r^2}{E_f f'_c + k_e f_1} \quad (22)$$

378 Fig. 9 shows the variation in the parameter $\varepsilon_{cu} / \varepsilon_{co}$ with
 379 $\rho_f f_u / f'_c$ for the different cases examined, highlighting the
 380 importance of the shape of the cross-section in the ul-

381 timate deformation capacity in compression of a con-
 382 crete core confined by FRP.

5. Comparison between analytical and experimental results

385 In the present section some experimental results on
 386 the use of FRP materials for confining concrete, recently
 387 presented in the literature [3–13], are presented for
 388 comparison with analytical results.

389 The above-mentioned results regard compressive
 390 tests on prismatic and cylindrical specimens of different
 391 sizes, reinforced with different types of FRP materials
 392 (carbon, glass, aramid, etc.), with different concrete
 393 strengths. Tests on prismatic specimens regard members
 394 reinforced with carbon fiber and having a square cross-
 395 section with rounded corners with different radii r of the
 396 corner ($r = 3, 5, 25$ and 38 mm). In all tests, unidirectional
 397 fiber wraps with an anchorage length (generally
 398 between 50 and 100 mm) necessary to avoid sliding or
 399 debonding of fibers during the tests were utilized and
 400 rupture of fibers was always observed.

401 Table 1 gives average values for the cases mentioned
 402 [4,5,7–9,13]: dimensions and shapes of the specimens
 403 tested; mechanical characteristics and volumetric per-

Table 1
 Characteristics of specimens and materials tested

Code	Refs.	Concrete type				Mater.	FRP characteristics				
		b_d (mm)	r (mm)	f'_c (MPa)	ε_{co} (%)		t (mm)	ρ_f (%)	E_f (GPa)	ε_f (%)	f_u (MPa)
C1	[13]	100	0	20.05	0.207	Carbon	0.165	0.66	230	1.5	3430
SR1	[13]	100	3	20.05	0.207	Carbon	0.165	0.66	230	1.5	3430
C2	[3]	150	0	36.90	0.250	Carbon	0.167	0.44	235	1.5	3510
C3	[3]	150	0	36.90	0.250	Carbon	0.501	1.34	235	1.5	3510
C4	[3]	150	0	36.90	0.250	Glass	1.20	3.20	26	1.6	399
C5	[3]	150	0	36.90	0.250	Glass	3.60	9.60	26	1.6	399
C6	[7]	190.6	0	27.07	0.198	Carbon	0.22	0.46	230	1.5	3483
C7	[7]	190.6	0	27.07	0.198	Carbon	0.22	0.46	230	1.5	3483
C8	[5]	155	0	60.00 ^a	/	Carbon	0.13	0.33	230	1.5	3500
C9	[5]	155	0	60.00 ^a	/	Carbon	0.26	0.67	230	1.5	3500
C10	[5]	155	0	60.00 ^a	/	Carbon	0.39	1.00	230	1.5	3500
C11	[9]	100	0	42.00	/	Carbon	0.60	2.41	82.70	1.5	1265
C12	[9]	150	0	43.00	/	Aramid	1.26	3.93	13.60	1.69	230
C13	[9]	150	0	43.00	/	Aramid	2.52	6.83	13.60	1.69	230
C14	[9]	150	0	43.00	/	Aramid	3.78	10.30	13.60	1.69	230
C15	[9]	150	0	43.00	/	Aramid	5.04	13.90	13.60	1.69	230
SR2	[9]	152	5	43.90	/	Carbon	1.50	3.93	82.70	1.5	1265
SR3	[9]	152	25	43.90	/	Carbon	1.50	3.79	82.70	1.5	1265
SR4	[9]	152	38	35.80	/	Carbon	1.50	3.76	82.70	1.5	1265
SR5	[9]	152	38	42.00	/	Carbon	1.50	2.25	82.70	1.5	1265
C16	[8]	300	0	32.00	0.250	Carbon	0.30	0.40	84.00	1.5	1770
C17	[8]	300	0	44.00	0.270	Carbon	0.30	0.40	84.00	1.5	1770
C18	[8]	300	0	44.00	0.270	Carbon	0.90	1.20	84.00	1.5	1770
S1	[8]	300	0	32.00	0.250	Carbon	0.90	1.20	84.00	1.5	1770

C = circular; S = square; SR = square with circular corners.

^a Determined on cube 150×150 mm².

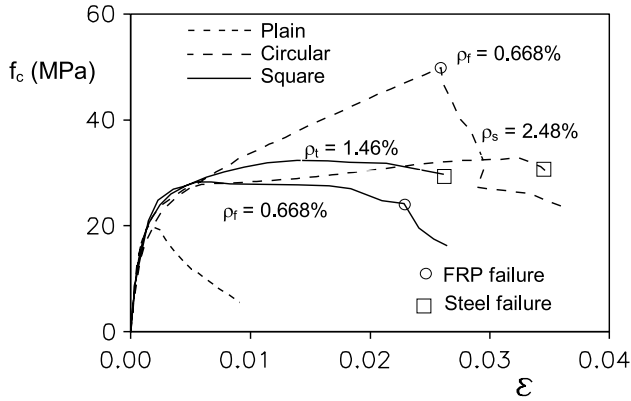


Fig. 10. Stress–strain curves for 100 × 200 mm² concrete specimens confined with CFRP and/or transverse steel reinforcements.

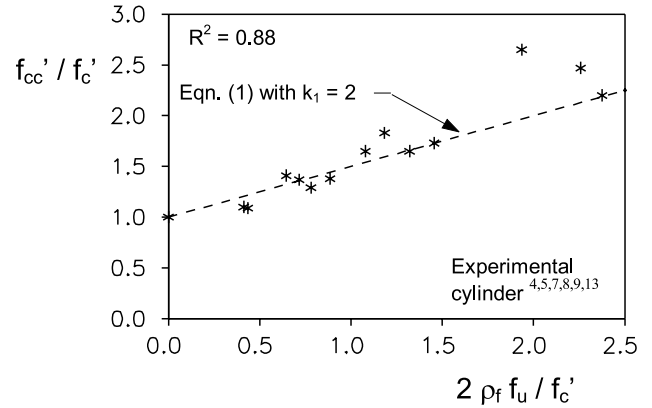


Fig. 13. Variation in compressive strength with $2\rho_f f_u / f'_c$.

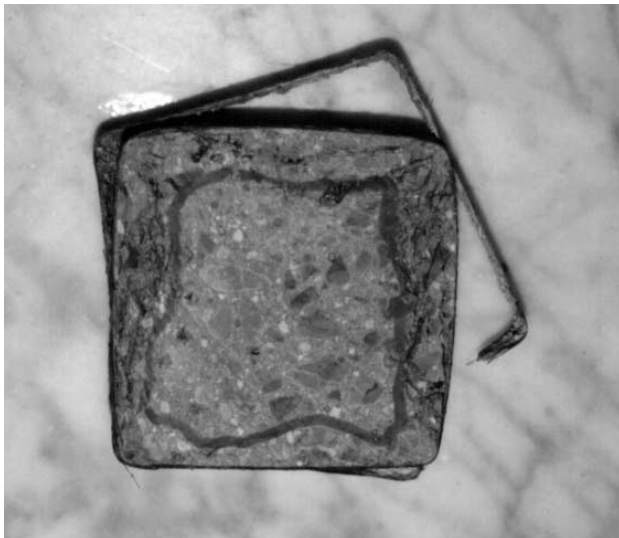


Fig. 11. Transverse cross-section of compressed concrete members with square section confined with FRP at failure [13].

centages of fibers utilized; mechanical properties of unconfined concrete. 404 405

Of particular interest is the experimental investigation of Rochette [9] in which the influence of the shape of the cross-section and the types and volumetric percentage of fibers on the compressive behavior of concrete members reinforced with FRP was examined. In the same investigation the strain in FRP was also recorded during the tests, and based on these results it was possible to calibrate the k_i factor. 406 407 408 409 410 411 412 413

It emerges from all the mentioned experimental investigations that the use of FRP produces a significant change in the behavior of plain concrete in terms of both maximum strength and strain. In particular, a significant increase in maximum strength was observed for the circular cross-section; instead less effective confinement was observed for square sections or square sections with round corners. This is due to the intensification of stresses at the corners and consequently to the lower confining pressure and smaller effective concrete core area. These aspects are also confirmed by experimental research carried out by Campione et al. [13]. 414 415 416 417 418 419 420 421 422 423 424 425

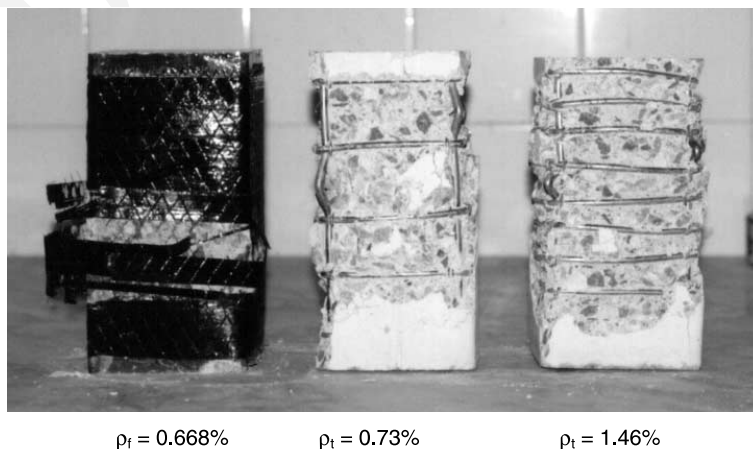


Fig. 12. Mode of failure of concrete specimens reinforced with transverse steel reinforcement and FRP [13].

Table 2
Mechanical properties of tested specimens

Code	Experimental values				Analytical values			
	f'_{cc} (MPa)	f'_{cc}/f'_c	ϵ_{cu} (%)	ϵ_{cf} (%)	f'_{cc} (MPa) (1)	f'_{cc}/f'_c	ϵ_{cu} (%) (21)	ϵ_{cf} (%)
C1	49.60	2.47	2.55	/	42.69	2.13	1.07	/
SR1	31.15	1.55	2.25	/	21.91	1.09	0.64	0.29
C2	47.60	1.29	0.80	/	52.53	1.42	0.77	/
C3	81.10	2.20	1.40	/	83.79	2.27	1.41	/
C4	52.30	1.41	1.80	/	49.67	1.34	0.70	/
C5	98.00	2.65	3.20	/	75.20	2.04	1.30	/
C6	53.89	1.99	0.57	/	43.15	1.59	0.94	/
C7	49.62	1.83	0.49	/	43.15	1.59	0.94	/
C8	54.27	1.09	0.77	/	61.54	1.23	0.57	/
C9	68.76	1.38	1.47	/	73.28	1.47	0.83	/
C10	82.27	1.65	1.75	/	85.03	1.71	1.04	/
C11	73.50	1.75	1.60	/	72.36	1.73	1.06	/
C12	47.30	1.10	1.11	/	50.73	1.18	0.53	/
C13	58.91	1.37	1.47	1.53	58.45	1.36	0.76	1.50
C14	70.95	1.65	1.69	/	66.18	1.54	0.96	/
C15	74.39	1.73	1.74	/	73.91	1.72	1.14	/
SR2	43.90	1.00	1.02	0.44	47.29	1.09	0.32	0.33
SR3	47.85	1.09	0.90	0.51	57.85	1.34	0.51	0.65
SR4	68.73	1.92	2.39	0.86	66.65	1.55	0.68	0.87
SR5	47.46	1.13	1.08	/	45.32	1.08	0.77	/
C16	40.00	1.25	0.66	/	39.08	1.22	0.56	/
C17	48.00	1.09	0.97	/	51.08	1.16	0.56	/
C18	75.00	1.70	1.82	/	66.24	1.50	1.06	/
S1	35.00	1.09	1.00	/	33.06	1.03	0.58	/

C = circular; S = square; SR = square with circular corners.

426 In this connection, Fig. 10 shows typical stress–strain
427 curves for concrete specimens with circular sections or
428 square sections with round corners tested in compression.

429 For a comparison the same figure shows results related
430 to concrete specimens confined with traditional
431 steel reinforcement constituted by spirals or stirrups with
432 volume percentage ρ_s for spirals and ρ_t for stirrups. The
433 objective of this comparison was to show, for the same
434 concrete bath, the confinement effects of FRP in terms of
435 both maximum stress and strain capacities with respect
436 to those obtained utilizing traditional transverse steel
437 reinforcement, that is very often difficult to place in cast
438 due to the high percentages required in critical regions.

439 Figs. 11 and 12 show the condition of prismatic
440 specimens tested by Campione et al. [13] after failure
441 occurs. Fig. 11 is related to the transverse cross-section
442 and shows the effective concrete core and FRP failure at
443 the corner, Fig. 12 shows the full specimens and compares
444 the effect of the confinement due to traditional steel
445 steel reinforcements with that produced by FRP. The
446 presence of FRP, up to its failure in tension, also avoids
447 the cover expulsion, like instead does not occur if traditional
448 transverse steel reinforcement is utilized.

449 Fig. 13 shows the variation in the increase in maximum
450 strength with $2\rho_f f_u / f'_c$ for members having a circular
451 cross-section. The experimental data [4–13] are

almost all mentioned in Fig. 13; in Table 1 are given
only average values.

The results confirm that the variation in strength can be
assumed linearly variable with the effective lateral pressure.
In particular, for cylindrical specimens utilizing, in
(1) $k_1 = 2$, a correlation factor R^2 of 88% was obtained.
In the regression analysis utilized, to obtain $k_1 = 2$ it was also
assumed that the intercept of the straight line f'_{cc}/f'_c is
equal to one if $2\rho_f f_u / f'_c$ is equal to zero. In the case of
specimens having transverse cross-section square and
square with round corners same coefficient $k_1 = 2$ can also

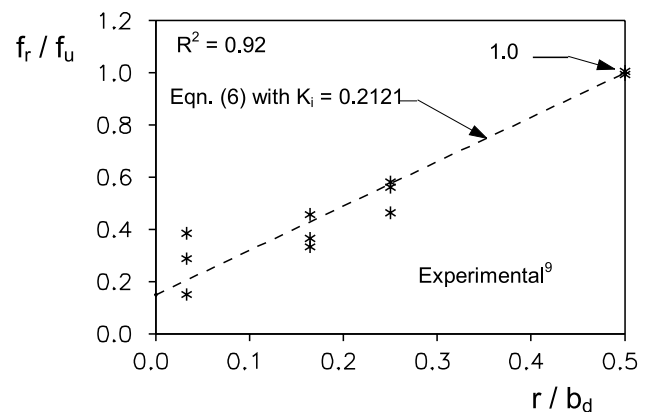


Fig. 14. Variation in effective stress in FRP with r/b_d .

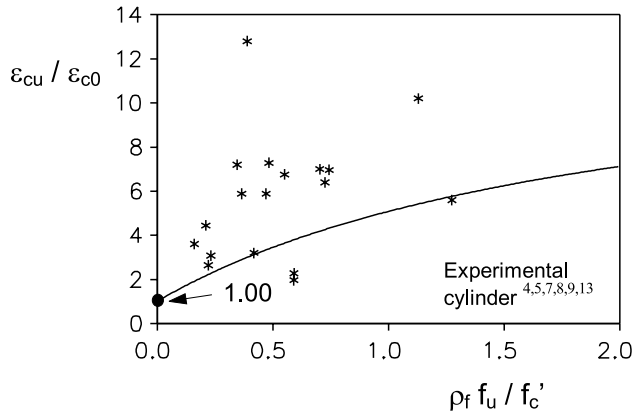


Fig. 15. Variation in ultimate strain of concrete core with $\rho_f f_u / f'_c$.

463 be assumed and good agreement with experimental data is
464 obtained, like shown in Table 2.

465 Fig. 14 shows the variation in the f_r stress in FRP with the
466 variation in r/b_d obtained using (5) and compared with the
467 experimental values mentioned in Rochette et al. [9]. In this case
468 too the assumption of a linear variation of f_r with r/b_d can be
469 considered reasonable and the k_i parameter can be assumed to
470 be constant and equal to 0.2121. This coefficient calibrated on
471 the basis of the total number of specimens examined in the lit-
472 erature [9] was obtained utilizing a regression analysis with
473 $R^2 = 92\%$ and considering that the intercept of the straight line
474 f_r/f_u is equal to one if r/b_d is equal to 1/2.

475 Fig. 15 shows the variation in maximum strain ε_{cu} ,
476 obtained by using (18) for the cases of members having a
477 circular cross-section, with the parameter $\rho_f f_u / f'_c$. The
478 figure reproduces almost all cases given in the mentioned
479 literature [4,5,7–9,13]; instead, only average values are
480 given in Table 2.

481 The results show that the analytical model to derive
482 ε_{cu} is very conservative; this can be justified by consid-
483 ering that the model is derived in a simplified and con-
484 servative hypothesis. As mentioned before, the strain
485 values obtained are very conservative, but it can be ac-
486 cepted by considering that the experimental data utilized
487 for comparison are related to small size specimens and if
488 also size effects smaller ultimate strain values are ex-
489 pected. Table 2, as already mentioned, gives the theo-
490 retical and experimental results related to the cases
491 mentioned in Table 1. Comparison between experi-
492 mental and analytical values shows good agreement.

493 Fig. 16, compares the experimental stress–strain
494 curve recorded in compression by Rochette et al. [9] with
495 that obtained using (11). In particular results relative to
496 specimens having circular (specimen C11) and square
497 section with round corners with $r = 38$ mm (specimen
498 SR5) were mentioned showing good agreement for both
499 cases and stressing that the proposed model allows one
500 to predict accurately the experimental response.

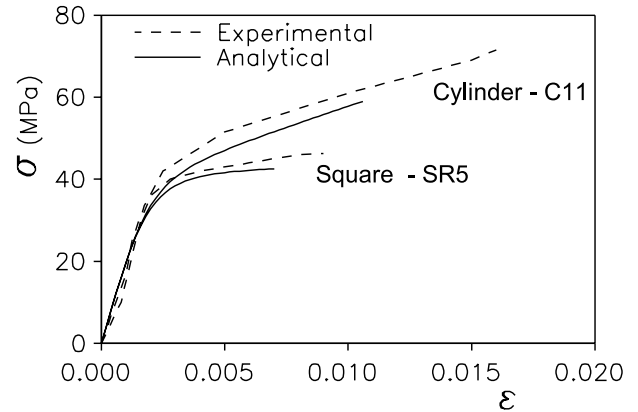


Fig. 16. Experimental and analytical comparison of stress–strain curves in compression according to data of Rochette et al. [9].

6. Conclusions

501

502 An analytical model to predict the maximum strength
503 and the maximum strain of concrete compressed mem-
504 bers reinforced with FRP has been presented. The in-
505 fluence of the shape of the transverse cross-section
506 (circular, square and square with round corners) on the
507 compressive behavior of members is examined.

The model allows one to obtain:

508

- the strength of the compressed members referring to
the effective confined core depending on the shape
of the cross-section; 510 511
- the reduced confining pressure in a square section
with circular corners due to the concentration of
stresses at the corners. 513 514

515 The proposed model also allows one to evaluate ul-
516 timate strain in the concrete core based on a simplified
517 energetic approach for whose application only the geo-
518 metrical and mechanical characteristics of FRP and the
519 maximum strengths of unconfined and confined con-
520 crete are required.

521 The complete stress–strain relationship proposed for
522 FRP confined concrete permits one to accurately re-
523 produce the behavior of concrete members reinforced
524 with FRP in agreement with the available experimental
525 data.

526 Finally, further studies are required to validate the
527 proposed equations if size effects have to be taken into
528 account and if failure of concrete specimens also occurs
529 when FRP does not fail in tension.

References

530

- [1] Mander JB, Priestley MJN, Park R. Theoretical stress–strain
model for confined concrete. ASCE J Struct Eng
1988;114(8):1804–26. 531 532 533
- [2] Cusson D, Paultre P. Stress–strain model for confined high
strength concrete. ASCE J Struct Eng 1995;121(3):468–77. 534 535

- 536 [3] Arduini M, Di Tommaso A, Manfroni O, Ferrari S, Romagnolo
537 M. Il confinamento passivo di elementi compressi in calcestruzzo
538 con fogli di materiale composito. *Industria Italiana del Cemento*
539 1999;11:836–41 (in Italian).
- 540 [4] Arduini M, Di Tommaso A, Mantegazza G. Compositi per la
541 riabilitazione strutturale. *Atti delle Giornate AICAP 97*
542 1997;1:29–240 (in Italian).
- 543 [5] Bortolotti L, Lai S, Carta S, Cireddu D. Comportamento a carico
544 assiale di conglomerati ad alta resistenza confinati con tessuto di
545 fibra di carbonio. *Atti delle Giornate AICAP 99* 1999;1:5–14 (in
546 Italian).
- 547 [6] Mirmiran A, Shahawy M. Behavior of concrete columns confined
548 by fiber composites. *ASCE J Struct Eng* 1997;123(5):583–90.
- 549 [7] Purba BK, Mufti AA. Investigation of the behaviour of circular
550 concrete columns reinforced with carbon fiber-reinforced polymer
551 (CFRP) jackets. *Can J Civ Eng* 1999;26:590–6.
- 552 [8] Demers M, Neale WK. Confinement of reinforced concrete
553 columns with fibre-reinforced composite sheets – an experimental
554 study. *Can J Civ Eng* 1999;26:26–241.
- [9] Rochette P, Labossière P. Axial testing of rectangular column
models confined with composites. *ASCE J Comp Construct*
2000;4(3):129–36.
- [10] Saadatmanesh H, Ehsani MR, Li MW. Strength and ductility of
concrete columns externally reinforced with fiber composite
straps. *ACI Struct J* 1994;91(4):434–47.
- [11] Saafi M, Toutanji HA, Li Z. Behavior of concrete columns
confined with fiber reinforced polymer tubes. *ACI Mater J*
1999;96(4):500–9.
- [12] Seible F, Priesley MJN, Hegemier GA, Innamorato D. Seismic
retrofit of R.C. columns with continuous carbon fiber jackets.
ASCE J Compos Construct 1997;1(2):52–62.
- [13] Campione G, Miraglia N, Scibilia N. Comportamento in com-
pressione di elementi in calcestruzzo armato a sezione quadrata e
circolare rinforzati con FRP. *Ingegneria Sismica* 2001;2 (in
Italian).
- [14] Pinto PE, Giuffrè A. Comportamento del cemento armato per
sollecitazioni cicliche di forte intensità. *Giornale del Genio Civile*
1970;5 (in Italian).

555
556
557
558
559
560
561
562
563
564
565
566
567
568
569
570
571
572
573